

SIMULATION MODEL OF *CRYPTOMONAS OVATA* POPULATION DYNAMICS IN SOUTHERN KOOTENAY LAKE, BRITISH COLUMBIA

JAMES E. CLOERN

Department of Zoology, Washington State University, Pullman, Wash. (U.S.A.)

Present address: U.S. Geological Survey, Water Resources Division, 345 Middlefield Road, Menlo Park, Calif. 94025 (U.S.A.)

(Received 6 November 1976; revised 1 March 1977)

ABSTRACT

Cloern, J.E., 1978. Simulation model of *Cryptomonas ovata* population dynamics in southern Kootenay Lake, British Columbia. *Ecol. Modelling*, 4: 133—149.

A one-dimensional transient model is developed to simulate observed population dynamics of a small flagellate (*Cryptomonas ovata*) in southern Kootenay Lake, B.C., during a 1-year period (1 June 1974—31 May 1975). The model considers advective displacement of *C. ovata* as water flows from its southern entrance into the lake and moves northward toward sampling sites. Specific growth rate is computed from an experimentally determined function of mean irradiance, water temperature, and nutrient (ammonium and phosphate) concentration in the upper 10 m of the water column. Cell losses are assumed to result from zooplankton grazing and inhibition due to presence of the blue-green alga *Anabaena*.

The model simulates well the timing and magnitude of all observed population changes and, more importantly, it gives insight into the important mechanisms which regulate population density of *C. ovata* in this natural system.

INTRODUCTION

One of the most intriguing problems facing aquatic ecologists is the challenge to develop a realistic and precise simulation model of phytoplankton population dynamics, species composition, and primary productivity. Most previous attempts to simulate algal population dynamics have treated the phytoplankton as a homogeneous unit. However, recent studies have begun to stress the very real physiological differences which exist among phytoplankton species. Perhaps the most realistic simulation approach is to treat each species separately and deal with its particular response to changing environments. Although this approach requires species-specific kinetic information, the output of such models will be valuable in explaining natural phenomena like seasonal succession; and since each algal species is utilized to a different degree by organisms at higher trophic levels, it may also lead to

more realistic simulations of secondary productivity. This rationale motivated development of the following model to simulate population dynamics of one important phytoplankter (*Cryptomonas ouata*) in southern Kootenay Lake, British Columbia.

LIMNOLOGY OF SOUTHERN KOOTENAY LAKE

The main body of Kootenay Lake occupies part of the Purcell Trench located in southeastern British Columbia (Fig. 1). Its main axis runs north-south for approximately 105 km, its mean depth is 109 m, and maximum width is 6.4 km. The main basin is drained by a shallower west arm, and its major influent is the Kootenay River which enters from the south and contributes about 80% of total inflow (Northcote, 1972). This lake has been of particular interest during the past 25 years because it experienced a temporary but dramatic increase in phosphate loading. Recent limnological changes have been documented by Zyblut (1970), Taylor (1972), Northcote (1972, 1973), Davis (1973), and Cloern (1976a). Parker (1973, 1976) has developed a detailed simulation model of the lake's plankton populations and water chemistry.

Past studies have emphasized the Kootenay River's role in dominating the physical and biological nature of Kootenay Lake. Consequently, this investigation was concentrated on that part of the lake which is most directly influ-

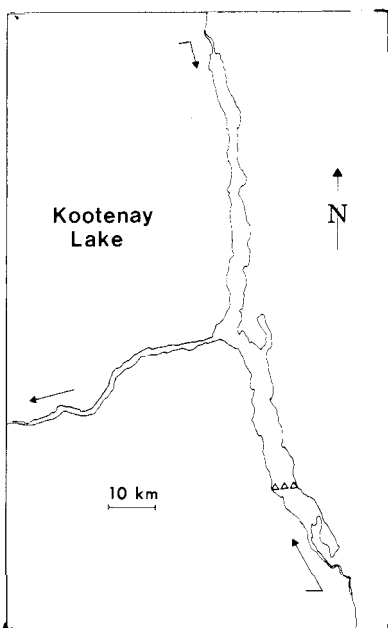


Fig. 1. Map of Kootenay Lake showing the location of sampling stations (triangles).

enced by the river — i.e., the southern arm. A 1-year study of southern Kootenay Lake defined the temporal changes in those driving variables (water chemistry, irradiance, temperature, and plankton composition) which most significantly affect phytoplankton population development. A detailed description of this study is given elsewhere (Cloern, 1976a). Briefly, three sampling stations were selected along an east—west transect located about 11 km from the mouth of the Kootenay River (Fig. 1). At each station, water samples were collected at depths of 1, 5, and 10 m. These were analyzed in the laboratory for nitrate, ammonium, and reactive phosphate concentrations. Similar water samples taken from each depth at each station were preserved and returned to the laboratory for phytoplankton enumeration. Zooplankton tows were also taken at the three stations and depths. Water temperature and light intensity were measured at 1-m intervals from the surface to 10 m, and profiles of irradiance in the water column were used to estimate the coefficient of light extinction (Hutchinson, 1957) at each station.

Southern Kootenay Lake was sampled on 22 dates between 6 June 1974 and 15 May 1975. Results are given as a mean of pooled measurements taken from all three depths at all three stations, and therefore represent mean values associated with the upper 10 m of the water column for each sampling date. Daily estimates of all measured variables were obtained for the simulated year with a bicubic-spline interpolation routine (IMSL Library 1, 1975), and these results are shown in Figs. 2—7.

Nutrients

Mean nitrate concentrations fluctuated erratically in southern Kootenay Lake (Fig. 2), particularly during the spring months when runoff and Kootenay River discharge were high. Ammonium concentrations also varied during the spring and then stabilized at about $1 \mu\text{M}$ after September. Total inorganic nitrogen (ammonium plus nitrate) never fell below $3 \mu\text{M}$ and was often above $5 \mu\text{M}$ (Fig. 2). Total soluble phosphate concentrations changed dramatically throughout the year (Fig. 3) and varied between 0.0 and $0.95 \mu\text{M}$.

Plankton

Total filter-feeding zooplankton density exhibited three major peaks between June and October 1974 (Fig. 4). The first peak was exclusively *Diatomus ashlandi*. The August—September peak comprised mainly *Diatomus* and *Diaphanosoma leuchtenbergianum*, and a third peak included these two species plus smaller populations of *Daphnia galeata* and *Bosmina coregoni*.

The species composition and population densities of southern Kootenay Lake's phytoplankton are detailed in Cloern (1976a). Changes in population

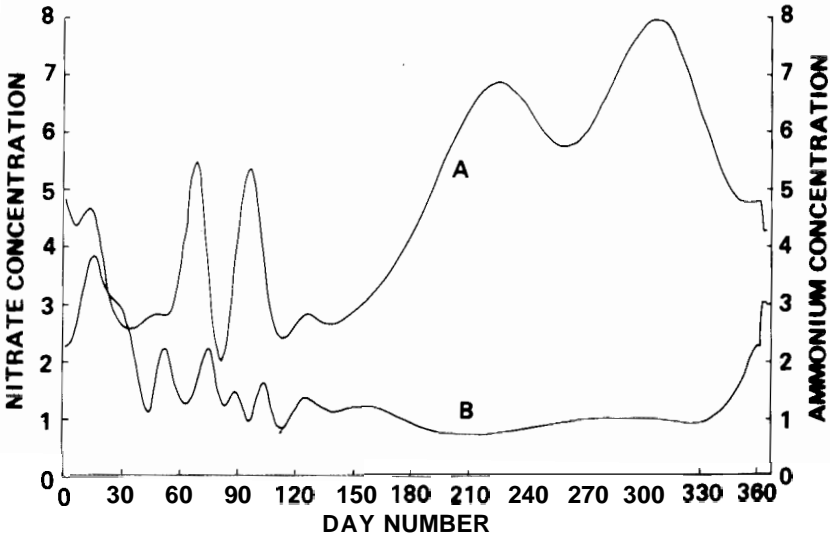


Fig. 2. Daily estimates of mean ammonium (A) and nitrate (B) concentration (μM) in the upper 10 m of southern Kootenay Lake. Day 1 = 1 June 1974.

density of the two *Anabaena* species (*A. circinalis* and *A. macrospora*) are given here (Fig. 5) since this blue-green genus may inhibit growth of *Cryptomonas ovata* (see below). Total *Anabaena* density exhibited two peaks during the summer—fall of 1974. The first peak (around day 70) was almost exclusively *A. circinalis* and the later peak (around day 110) was mostly *A. macrospora*.

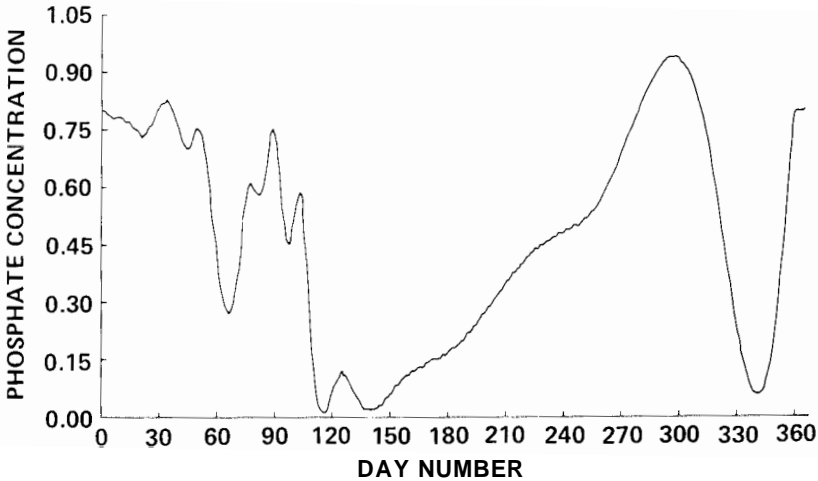


Fig. 3. Daily estimates of mean soluble phosphate concentration (μM) in the upper 10 m of southern Kootenay Lake. Day 1 = 1 June 1974.

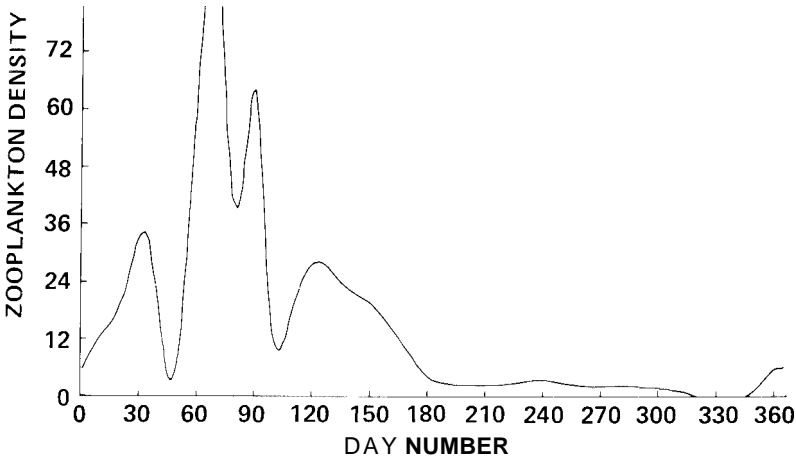


Fig. 4. Daily estimates of total filter-feeding zooplankton density (number of animals/l) in the upper 10 m of southern Kootenay Lake. Species included are *Diaptomus ashlandi*, *Diaphanosoma leuchtenbergianum*, *Daphnia galeata*, and *Bosmina coregoni*. Day 1 = 1 June 1974.

Physical parameters

Only slight temperature differences were found between stations, and the upper 10 m of southern Kootenay Lake were homothermic on most sampling dates. Mean water temperature increased during June and July 1974, reached a maximum of 20°C in August, and then declined gradually

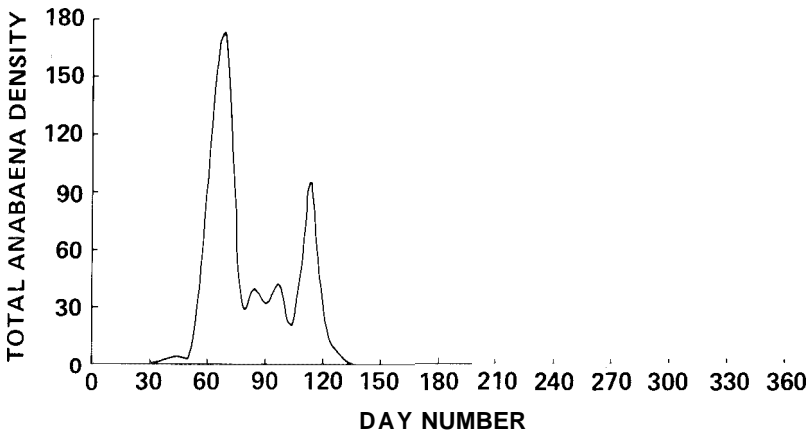


Fig. 5. Daily estimates of *Anabaena circinalis* plus *Anabaena macrospora* density (number of filaments/ml) in the upper 10 m of southern Kootenay Lake. Day 1 = 1 June 1974.

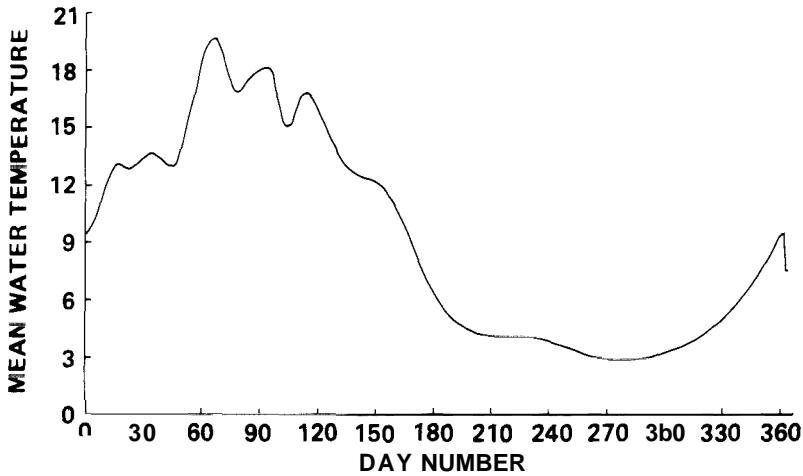


Fig. 6. Daily estimates of mean water temperature ($^{\circ}\text{C}$) in the upper 10 m of southern Kootenay Lake. Day 1 = 1 June 1974.

to a winter minimum of 3°C in March 1975 (Fig. 6). Water clarity (measured as extinction coefficient) changed dramatically throughout the year (Fig. 7). Spring months were characterized by very high turbidity resulting from the large silt load during maximum Kootenay River discharge. As river discharge declined, water clarity increased through the summer and fall and reached a maximum in March 1975.

Daily insolation and photoperiod were estimated with a sub-model since continuous meteorological data are not collected near Kootenay Lake. Total clear-sky solar radiation incident to the earth's surface is given by the

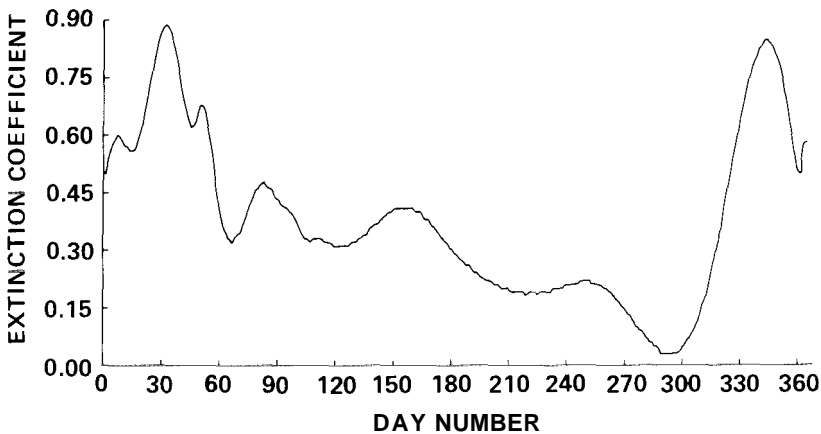


Fig. 7. Daily estimates of light-extinction coefficient (m^{-1}) in the upper 10 m of southern Kootenay Lake. Day 1 = 1 June 1974.

Milankovitch equation (List, 1958):

$$I_0 = \frac{S_0}{r} \int_{t_1}^{t_2} \alpha^{\sec Z_a} \cdot \cos Z_a dt, \quad (1)$$

where I_0 is in ly/day, S_0 is the solar constant (1.94 ly/min), r is the earth-to-sun separation, t_1 is time of sunrise, t_2 is time of sunset, α is the atmospheric transmission coefficient, and Z_a is solar zenith angle. Z_a , r , t_1 , and t_2 can be computed for any day of the year at any given latitude ($49^\circ 20'$ for southern Kootenay Lake) by the methods of McCullough and Porter (1971).

Assuming that a is 0.84 (Huang and Park, 1975), total clear-sky insolation was computed for every day of the simulated year by numerically integrating Eq. (1).

Clear-sky radiation was corrected for cloud cover with the formula of Berliand (Huang and Park, 1975):

$$I_c = (1 - 0.386 \cdot C - 0.36 \cdot C^2) \cdot I_0, \quad (2)$$

where C is mean monthly cloudiness (Monthly Record, 1974, 1975). The diffuse component (I_d) of solar radiation was assumed to be a function of the incident component (Parker, 1973):

$$I_d = (0.054 + 0.07 \cdot a \cdot \exp(0.226 \cdot Z_a^{4.72})) \cdot I_c, \quad (3)$$

where a is albedo (0.1 over water). Total daily insolation is then the sum of (2) and (3).

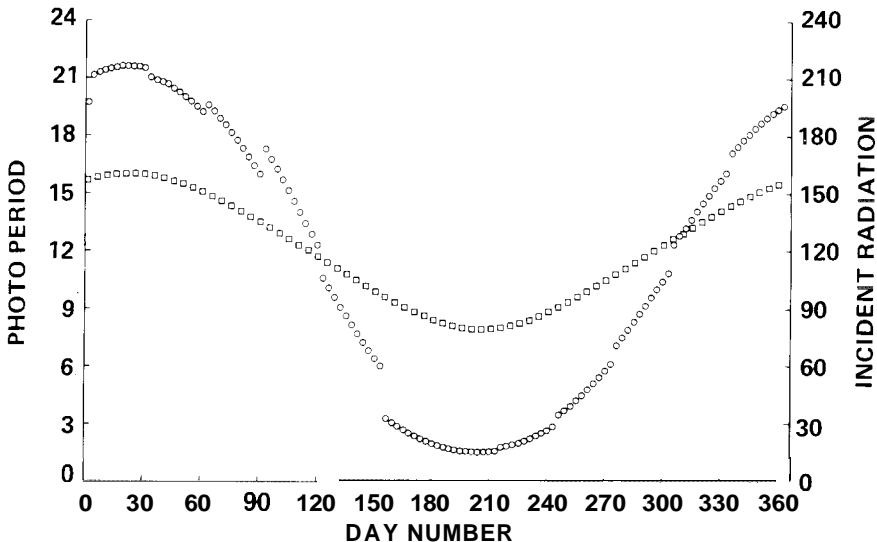


Fig. 8. Hours of sunlight (photoperiod = \square) and total daily insolation (\circ), 400–700 nm, reaching the surface of southern Kootenay Lake. Day 1 = 1 June 1974.

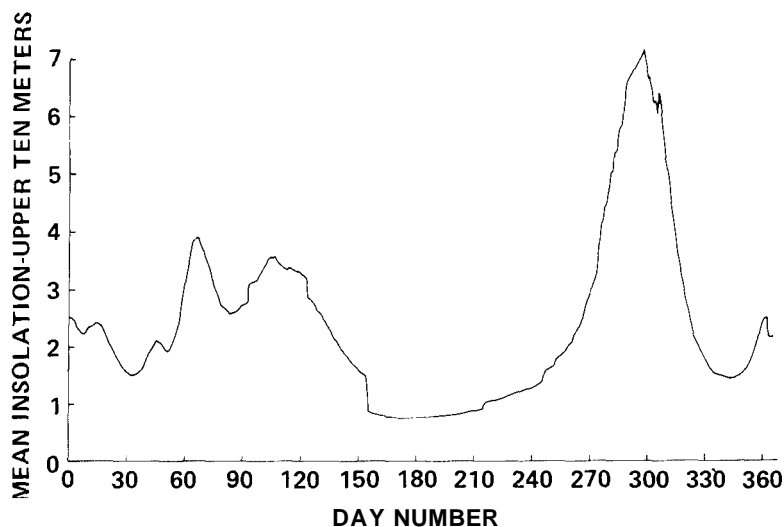


Fig. 9. Daily estimates of mean insolation (ly/h) in the upper 10 m of southern Kootenay Lake. Day 1 = 1 June 1974.

Assuming that photosynthetically useable radiation includes those wavelengths between 400 and 700 nm, daily useable insolation incident to Kootenay Lake was computed as:

$$I_s = 0.41 \cdot (I_c + I_d), \quad (4)$$

where the fraction 0.41 is from List (1958). Daily estimates of I_s and photo-period (PP = number of daylight hours per 24 h) are shown in Fig. 8.

Light intensity at depth z is determined by mean surface irradiance and extinction coefficient (k) of the water column:

$$I_z = \frac{I_s}{PP} \cdot \exp(-k \cdot z), \quad (5)$$

and mean light intensity (ly/h) in the upper 10 m is then:

$$I_m = \frac{I_s}{10 \cdot PP} \int_0^{10m} \exp(-k \cdot z) dz. \quad (6)$$

Daily estimates of I_m are shown in Fig. 9.

GROWTH KINETICS OF *CRYPTOMONAS OVATA*

Laboratory experiments with batch cultures of *Cryptomonas ovata* var. *palustris* (obtained from the Indiana University Culture Collection of Algae) have defined the growth rate of this organism in response to irradiance, temperature, and nutritional state (Cloern, 1976b), where nutritional state is

defined as intracellular quantities of nitrogen and phosphorus. The specific growth rate of *C. ovata* is defined by the following function of irradiance and temperature:

$$\mu' = \mu_m(T) \cdot \frac{I}{I_{opt}(T)} \cdot \exp(1 - I/I_{opt}(T)), \quad (7)$$

where μ' has units day^{-1} , T is temperature ($^{\circ}\text{C}$), and I is photosynthetically useable irradiance (ly/h). Eq. (7) is Steele's (1965) empirical relation describing growth rate as a function of light intensity, modified by the observation that maximum specific growth rate (μ_m) and optimum irradiance (I_{opt}) both are exponential functions of temperature (Cloern, 1976b):

$$\mu_m(T) = 0.02 \cdot \exp(0.17 \cdot T) \quad (8)$$

$$I_{opt}(T) = 0.06 \cdot \exp(0.22 \cdot T). \quad (9)$$

When algal cells become nutrient-limited (usually by limited availability of nitrogen or phosphorus), their growth rate is smaller than that given by Eq. (7). Laboratory studies (e.g. Droop, 1968; Caperon and Meyer, 1972; Rhee, 1973) have shown that growth rate is determined by intracellular nutrient quantities, and the following function has been used to define this relationship:

$$\mu = \mu' \cdot \frac{q - q_0}{q}, \quad (10)$$

where q is internal quota ($\mu\text{mol}/10^6$ cells) of limiting nutrient, and q_0 is a minimum maintenance level of that nutrient. Maintenance levels of nitrogen (q_{0N}) and phosphorus (q_{0P}) were measured as $0.36 \mu\text{mol N}/10^6$ cells and $0.0035 \mu\text{mol P}/10^6$ cells for *Cryptomonas ovata* (Cloern, 1976b).

Computation of specific growth rate then requires a measure of internal nitrogen and phosphorus quotas (q_N and q_P). These can be estimated if the kinetics of inorganic nitrogen and phosphorus uptake are known. Absorption of nitrogen and phosphorus by algal cells is generally described by an expression that is analogous to Michaelis–Menten enzyme kinetics:

$$V = \frac{dq}{dt} = \frac{V_m \cdot S}{K_s + S}, \quad (11)$$

where V_m is the maximum uptake rate, K_s is the half-saturation constant, and S is nutrient concentration in the surrounding medium. The parameters V_m and K_s were measured in the laboratory to define the kinetics of nitrate, ammonium, and phosphate absorption by *Cryptomonas ovata* var. *palustris* in a varying regime of light intensities and temperatures (Cloern, 1976b). Mean maximum uptake rate of ammonium (V_{mN}) was $0.034 \mu\text{mol N}/10^5$ cells-h, and the mean half-saturation constant (K_{sN}) was $0.76 \mu\text{M}$ ammonium. Phosphate-uptake kinetic parameters were: $V_{mP} = 0.0004 \mu\text{mol P}/10^6$ cells-h, and $K_{sP} = 0.84 \mu\text{M}$ phosphate. Nitrate uptake proceeded at a very

slow rate in the presence of ammonium, thus suggesting that ammonium is the primary inorganic nitrogen source for *C. ovata* in Kootenay Lake. The nutritional state of *C. ovata* (q_N , q_P) can thus be approximated by integrating the rates of ammonium and phosphate uptake:

$$\frac{dq_N}{dt} = \frac{V_{mN} \cdot N_e}{K_{sN} + N_e} \quad (12)$$

$$\frac{dq_P}{dt} = \frac{V_{mP} \cdot P_e}{K_{sP} + P_e}, \quad (13)$$

where N_e and P_e are measured ammonium and phosphate concentrations.

Once nutritional state is defined, the reductions in growth rate resulting from nitrogen-limitation and phosphorus-limitation are given by:

$$r_N = \frac{q_N - q_{0N}}{q_N} \quad (14)$$

$$r_P = \frac{q_P - q_{0P}}{q_P}, \quad (15)$$

where r_N and r_P are relative growth rates (μ/μ'). Assuming that growth rate is limited by either phosphorus or nitrogen (but not both simultaneously) at any point in time, the reduction in growth rate resulting from nutrient-limitation is defined as:

$$r = \text{minimum of } (r_N, r_P). \quad (16)$$

Then specific growth rate (day^{-1}) at any given combination of irradiance, temperature, and nutritional state is

$$\mu = r \cdot \mu'. \quad (17)$$

THE MODEL

Since Kootenay Lake is a complex ecological system, a number of simplifying assumptions were made. In particular, the upper 10 m of southern Kootenay Lake were assumed to be well-mixed and to have homogeneous water chemistry, plankton density, and temperature. Although variability existed both with depth and among stations, this variability was not of sufficient magnitude to warrant use of a multi-dimensional spatial model. However, since the main inflow to Kootenay Lake is the Kootenay River entering from the south, and since there is considerable advective displacement of planktonic organisms as water flows from south to north, this hydrodynamic component had to be considered. The following model assumes a constant velocity of water flow from the mouth of the Kootenay River up the north-south axis of the lake, and that dispersion of plankton by turbulent eddy diffusion is small relative to advection in this system.

Given these assumptions, the population size of *Cryptomonas ovata* at any point along the north-south axis of Kootenay Lake and any point in time is governed by the following equation (e.g. DiToro et al., 1971):

$$\frac{\partial P}{\partial t} = G(t) \cdot P - V \cdot \frac{\partial P}{\partial X}, \quad (18)$$

where P is algal density (number of cells/ml), V is the assumed constant velocity of flow from south to north, X is distance from the mouth of the Kootenay River, and $G(t)$ is a time-variable net specific growth rate. Eq. (18) can be solved analytically if the initial and boundary conditions (defining $C. ovata$ density at the river mouth) are specified.

If inflow from the Kootenay River contributes "seed" organisms which initiate population development in the lake, then one might expect high population densities to enter southern Kootenay Lake when river flow is high (during spring months) and/or when environmental conditions are most conducive for growth (summer months). Similarly, one would expect small population densities at the river-lake boundary during the winter. The following boundary and initial conditions are consistent with this expected behavior and with observed population densities at the beginning of the simulated year:

$$\begin{aligned} \text{(a) } P_X(0) &= 20, & \text{all } X, t = 0. \\ \text{(b) } P_0(t) &= 20, & X = 0, t \leq 160 \\ P_0(t) &= P_0(t-1) - 0.3, & X = 0, 160 < t \leq 221 \\ P_0(t) &= 2, & X = 0, 221 < t \leq 344 \\ P_0(t) &= P_0(t-1) + 0.3, & X = 0, 344 < t \leq 365 \end{aligned}$$

Given these boundary conditions, the solution to Eq. (18) is (from A.R. Koch, personal communication, 1976):

$$P_X(t) = P_0(t - X/V) \cdot \exp \int_{(t-X/V)U_0}^t G(\tau) d\tau. \quad (19)$$

Note that the parameter X/V is a constant time delay associated with movement of a water mass from the mouth of the Kootenay River to point X up the lake. If $t \leq X/V$, $U_0 = 0$; and if $t > X/V$, $U_0 = 1$. Eq. (19) describes the population size of *Cryptomonas ovata* at the sampling stations if an integrable net growth rate function G is specified.

Net growth rate

Cryptomonas ovata's mean specific growth rate (day^{-1}) in the upper 10 m of the water column is defined as:

$$\bar{\mu} = \frac{1}{10 \text{ m}} \int_0^{10 \text{ m}} \frac{1}{15 \text{ h}} \int_0^{PP} \mu dt dz. \quad (20)$$

Note that integration with respect to time simply scales growth rate linearly to photoperiod (PP), and that laboratory measurements of $\mu_m(T)$ were based on a daily photoperiod of 15-h light per day. After integration, Eq. (20) becomes:

$$\bar{\mu} = \frac{\mu_m(T) \cdot PP}{150 \cdot k} \left[\exp \left(1 - \frac{\bar{I}}{I_{opt}(T)} \cdot \exp(-10 \cdot k) \right) - \exp \left(1 - \frac{\bar{I}}{I_{opt}(T)} \right) \right], \quad (21)$$

where \bar{I} is mean hourly irradiance reaching the surface of the lake ($= I_s/PP$).

Since net growth rate is the difference between this mean specific growth rate and specific death rate,

$$G(t) = \bar{\mu}(t) - d(t), \quad (22)$$

daily estimates of *C. ovata*'s loss rate are required. Zooplankton grazing is assumed to be a major cause of cell loss in Kootenay Lake. Although the filtering rate of crustacean zooplankters is a species-specific function of temperature and algal density, one can assume a constant filtering rate by all individuals for simplicity. Based upon the works of McMahan and Rigler (1965), Richman (1966), and Kibby (1971), an intermediate filtering rate of 1.8 ml/day was chosen to represent the grazing pressure by *Diaptomus*, *Diaphanosoma*, *Daphnia*, and *Bosmina*. The specific death rate of *C. ovata* due to grazing is then

$$d_{ZP} = 0.0018 \cdot ZP, \quad (23)$$

where d_{ZP} is specific loss rate (day^{-1}) of cells in a representative liter of the upper 10 m, and ZP is total number of zooplankters per liter.

Population density of *Cryptomonas ovata* exhibited a dramatic summer decline that was coincident with the appearance of *Anabaena circinalis* and *Anabaena macrospora*, and *C. ovata* initiated a fall population pulse only after these two blue-greens disappeared. Fogg (1962) and LeFèvre (1964) reviewed evidence that blue-greens may control the species composition of freshwater phytoplankton through their excretion of organic compounds, and Vance (1965) found that a blue-green (*Microcystis*) culture explicitly inhibited *C. ovata* growth. This evidence suggests that *Cryptomonas ovata*'s loss rate in Kootenay Lake may be directly proportional to the total density (number of filaments/ml) of *A. circinalis* and *A. macrospora* ($= BG$):

$$d_{BG} = \beta \cdot BG. \quad (24)$$

The coefficient β was estimated by taking that value ($\beta = 0.0015$) which produced the best fit between simulated and observed population dynamics. The specific death rate of *C. ovata* is then the combined loss rate from grazing and inhibition by *Anabaena*:

$$d = 0.0018 \cdot ZP + 0.0015 \cdot BG. \quad (25)$$

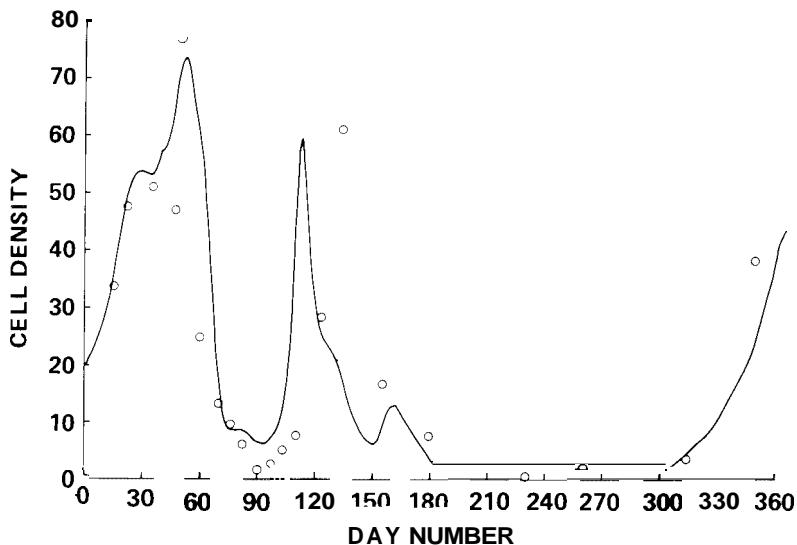


Fig. 10. Simulated (solid line) and observed (\circ) population densities (number of cells/ml) of *Cryptomonas ovata* in the upper 10 m of southern Kootenay Lake. Day 1 = 1 June 1974.

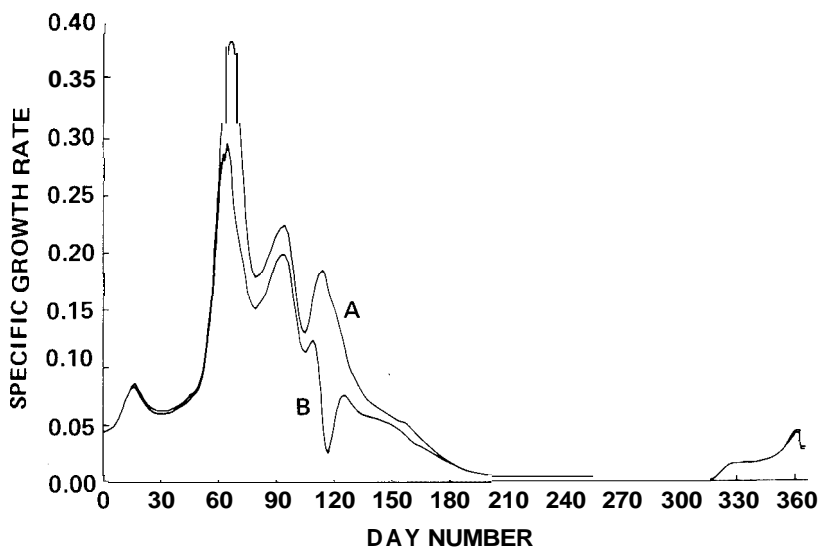


Fig. 11. Optimum growth rate (day^{-1}) of *Cryptomonas ovata* in the upper 10 m of southern Kootenay Lake (A), and the modified growth rate after incorporation of the nutrient-limitation effect (B). Day 1 = 1 June 1974.

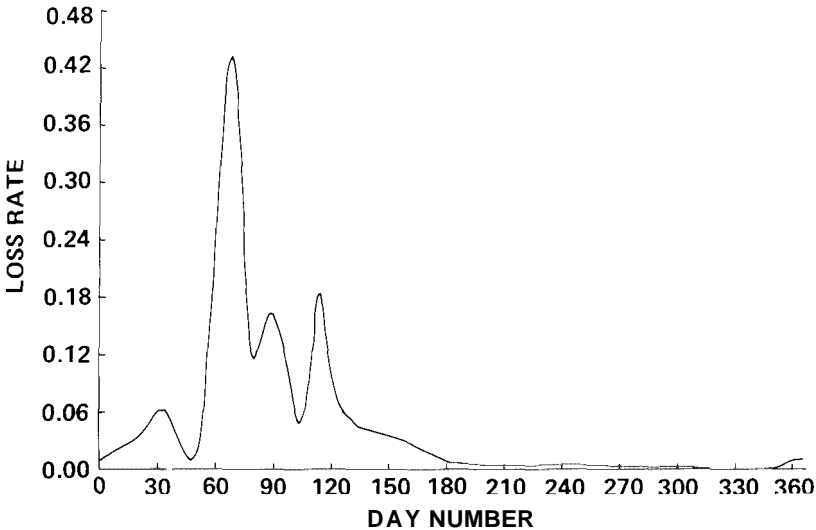


Fig. 12. Specific loss rate (day^{-1}) of *Cryptomonas ovata* in the upper 10 m of southern Kootenay Lake. Day 1 = 1 June 1974.

Model implementation

Although $G(t)$ is not in the form of a continuous analytic function, its required integral can be approximated as:

$$\int_a^b G dt \simeq \sum_{i=a}^b G_i, \quad (26)$$

where population growth has occurred in the time interval (a, b). Eq. (19) was solved (assuming a constant time-delay of $X/V = 40$ days) to give daily estimates of *C. ovata* population density at the sampling site. Results of this simulation are shown in Fig. 10 along with observed population densities. Fig. 11 compares optimum growth rates (Eq. (21)) with growth rates computed after incorporation of the nutrient-limitation effect (Eq. (17)). The difference between these two plots is a measure of the reduction in growth rate due to nutrient-limitation. Daily estimates of specific death rate are shown in Fig. 12.

DISCUSSION

The general behavior of this simulation model (Fig. 10) agrees well with observed population dynamics. The model predicts an early rapid population increase followed by a brief decline in growth, and then a population maximum around day 55. This early-summer maximum was followed by a rapid population decline that persisted until about day 110 (mid-September). At

this time *Cryptomonas ovata* exhibited an autumn pulse that lasted briefly and then declined to winter minimum levels. The reappearance of *C. ovata* during April and May 1975 is also simulated by the model. Both the timing and magnitude of all major population changes agree well between the simulated population and observed behavior. The lone exception is the model's failure to time accurately the autumn pulse.

The mechanisms underlying this complex population behavior are shown in Figs. 11 and 12. Note that specific growth rate was highest between days 55 and 125 (August—September) when water temperature (Fig. 6) and insolation (Fig. 9) were most conducive for growth. If the rate of cell division is proportional to photosynthetic rate, then this figure also represents annual changes in the specific rate of primary productivity by *C. ovata*. Population development was not limited by nutrient availability during the early part of the growing season (June—July) or during the winter months. However, growth rate was severely reduced by nutritional state in late September (days 110—130 in Fig. 11). This coincides with the period of very low dissolved phosphate concentrations seen in Kootenay Lake (Fig. 3), and suggests that phosphate-limitation contributed to the rapid decline of the autumn pulse.

Specific death rate was high during those same periods when growth rate was high — days 55—95 and 110—120 (Fig. 12). Loss rates corresponded to high zooplankton density (Fig. 4) and/or high blue-green density (Fig. 5), and the mid-summer decline of *C. ovata* is explained by the predominance of both zooplankton and *Anabaena*. Notice that both zooplankton and *Anabaena* densities reached relative minima around day 100, thus allowing for the increase in net growth rate that resulted in the autumn population peak. *Anabaena macrospora* reached high densities around day 115 (Fig. 5), and this reappearance coupled with phosphate limitation to cause the rapid decline of this autumn peak. The simulated third peak of *C. ovata* (day 155) occurred in response to the disappearance of both zooplankton and *Anabaena*, and to increased phosphate concentrations.

Population density of *C. ovata* was very small during the winter months because low water temperatures allowed for only small growth rates (Fig. 11), and because the Kootenay River was assumed to be bringing in fewer individuals. As water temperature increased, and as initial population densities from the river increased, *C. ovata* began a new annual cycle of growth during April and May 1975.

Although this model does a good job of simulating observed population dynamics, it can be improved with more detailed field data. In particular, the assumption of constant water velocity is unrealistic. Water velocities were periodically measured with drogues at the sampling stations and were found to vary erratically in both magnitude and direction (Parker, 1976). These measurements were not made often enough to elucidate any clear relationship between Kootenay River discharge and lake flow. However, since the Kootenay River exhibits dramatic changes in flow throughout the year

(Parker, 1976), one can reasonably assume that the river's flow regime significantly affects lake hydrodynamics near the sampling stations. Continuous monitoring of both river and lake flows would give the temporal changes in water velocity needed to make the model more realistic.

Further improvement would result from the measurement of *Cryptomonas ovata* population densities in the southern part of the lake. Water samples were periodically taken from the river's mouth and found to contain *Cryptomonas ovata*, but continuous sampling was not maintained. This information could have given a real measure of the river's role in providing an initial source of *C. ovata* throughout the year, and would have obviated the need for an arbitrary function of boundary population densities $P_0(t)$.

Laboratory measurement of Anabaena's effect on *Cryptomonas ovata* growth would also add veracity to the model. At this point, the assumption of a competitive interaction between these two algae is speculation. However, the inclusion of an Anabaena-effect was clearly necessary to mimic observed temporal changes in *Cryptomonas* density during the summer months. Simulated population changes do not match true population behavior when death rate is simply taken to be a result of zooplankton grazing. Both effects are necessary.

Even with these limitations, the model's output closely matches both the timing and magnitude of all major population changes. More importantly, the model offers valuable insight into the mechanisms which regulate the population dynamics of *Cryptomonas ovata* in a real system. It explains the temporal changes in specific growth rate (and hence primary productivity), and tells precisely when growth rate is limited by nutrient availability, light, and temperature. The model also gives a measure of cell losses from grazing, and this quantification of zooplankton grazing is a first step in describing energy flow from phytoplankton to zooplankton. The success of this effort will hopefully encourage further simulations at the species level.

ACKNOWLEDGEMENTS

I sincerely thank R.A. Parker and A.R. Koch for their assistance and guidance throughout this study. This project was funded by the Department of Zoology, Washington State University, and by Federal funds from the U.S. Environmental Protection Agency under grant number R-800430.

REFERENCES

- Caperon, J. and Meyer, J., 1972. Nitrogen-limited growth of marine phytoplankton. 1. Changes in population characteristics with steady-state growth rate. *Deep-sea Res.*, 19: 601–618.
- Cloern, J.E., 1976a. Recent limnological changes in southern Kootenay Lake, British Columbia. *Can. J. Zool.*, 54: 1571–1578.
- Cloern, J.E., 1976b. Population Dynamics of *Cryptomonas ovata*: A Laboratory, Field, and Computer Simulation Study. Thesis, Washington State Univ., Pullman, Wash., 102 pp.

- Davis, J.R., 1973. Effects of Reduced Inorganic Phosphate Income on Kootenay Lake, British Columbia. Thesis, Washington State Univ., Pullman, Wash., 47 pp.
- DiToro, D.M., O'Connor, D.J. and Thomann, R.V., 1971. A dynamic model of the phytoplankton populations in the Sacramento-San Joaquin Delta. *Adv. Chem. Ser.*, 106: 131—180.
- Droop, M.R., 1968. Vitamin B₁₂ and marine ecology. IV. The kinetics of uptake, growth, and inhibition in *Monochrysis lutheri*. *J. Mar. Biol. Assoc. U.K.*, 48: 689—733.
- Fogg, G.E., 1962. Extracellular products. In: R.A. Lewin (Editor), *Physiology and Biochemistry of Algae*. Academic Press, New York, N.Y., pp. 475—489.
- Huang, J.C. and Park, J.M., 1975. Effective cloudiness derived from ocean buoy data. *J. Appl. Meteorol.*, 14: 240—245.
- Hutchinson, G.E., 1957. *A Treatise on Limnology. I. Geography, Physics and Chemistry*. Wiley, New York, N.Y., 1015 pp.
- IMSL Library 1, 1975. *Computer Subroutine Libraries in Mathematics and Statistics*. IMSL Inc., Houston, Texas, 5th edn., 589 pp.
- Kibby, H.V., 1971. Energetics and population dynamics of *Diatomus gracilis*. *Ecol. Monogr.*, 41: 311—327.
- LeFèvre, M., 1964. Extracellular products of algae. In: D.F. Jackson (Editor), *Algae and Man*. Plenum Press, New York, N.Y., pp. 337—367.
- List, R.T., 1958. *Smithsonian Meteorological Tables*. Smithsonian Inst., Washington, D.C., 6th edn, 527 pp.
- McCullough, E.C. and Porter, W.P., 1971. Computing clear day solar radiation spectra for the terrestrial ecological environment. *Ecology*, 52: 1008—1015.
- McMahon, J.W. and Rigler, F.H., 1965. Feeding rate of *Daphnia magna* Strauss in different foods labeled with radioactive phosphorus. *Limnol. Oceanogr.*, 10: 105—113.
- Monthly Record, 1974. *Meteorological Observations in Canada*. Environment Canada, Downsview, Ont., 2304 pp.
- Monthly Record, 1975. *Meteorological Observations in Canada*. Environment Canada, Downsview, Ont., 2304 pp.
- Northcote, T.G., 1972. Some effects of mysid introduction and nutrient enrichment on a large oligotrophic lake and its salmonids. *Verh. Int. Ver. Limnol.*, 18: 1096—1106.
- Northcote, T.G., 1973. Some Impacts of Man on Kootenay Lake and Its Salmonids. *Great Lakes Fish. Comm. Tech. Rep.* 25, 46 pp.
- Parker, R.A., 1973. Some problems associated with computer simulation of an ecological system. In: M.S. Bartlett and R.W. Hiorns (Editors), *The Mathematical Theory of the Dynamics of Biological Populations*. Academic Press, London, pp. 269—288.
- Parker, R.A., 1976. *Phosphate Reduction and Response of Plankton Populations in Kootenay Lake*. U.S. Environmental Protection Agency, *Ecol. Res. Ser.*, 60013-76-063, 63 pp.
- Rhee, G-Y, 1973. A continuous culture study of phosphate uptake, growth rate and polyphosphate in *Scenedesmus* sp. *J. Phycol.*, 9: 495—506.
- Richman, S., 1966. The effect of phytoplankton concentration on the feeding rate of *Diatomus oregonensis*. *Verh. Int. Ver. Limnol.*, 16: 392—398.
- Steele, J.H., 1965. Notes on some theoretical problems in production ecology. In: C.R. Goldman (Editor), *Primary Production in Aquatic Environments*. *Mem. Ist. Idrobiol.*, 18 Suppl., Univ. California Press, Berkeley, Calif., pp. 385—398.
- Taylor, K.G., 1972. *Limnological Studies on Kootenay Lake*, British Columbia, Canada. Thesis, Washington State Univ., Pullman, Wash., 249 pp.
- Vance, B.D., 1965. Composition and succession of cyanophycean water blooms. *J. Phycol.*, 1: 81—86.
- Zyblut, E.R., 1970. Long-term changes in the limnology and macrozooplankton of a large British Columbia lake. *J. Fish. Res. Board Can.*, 27: 1239—1250.